

WHEN THE CONTINENTAL CRUST MELTS: A COMBINED STUDY OF MELT INCLUSIONS AND CLASSICAL PETROLOGY ON THE RONDA MIGMATITES

OMAR BARTOLI

Dipartimento di Scienze della Terra, Università di Parma, Viale Usberti 157/A, 43100 Parma, Italy

INTRODUCTION

Partial melting (anatexis) of the metasedimentary crust and melt extraction produce S-type granites in the upper crust and granitic leucosomes in migmatites, promoting chemical differentiation and weakening of the Earth's continental crust, with dramatic effects on tectonic processes, mountain building and geodynamics (Brown *et al.*, 2011; Sawyer *et al.*, 2011). Methods to directly determine the precise composition of the primary anatectic melt, including the nature and concentration of the dissolved volatiles, have not been previously described. Despite the fact that S-type granites and leucosomes provide important compositional information (Clemens, 2003; Sawyer, 2008), their nature as primary anatectic melts is questioned by several lines of evidence (Sawyer, 2008; Clemens & Stevens, 2012). Hence, the composition of primary melts and the fluid regime during the early stages of crustal anatexis have been assumed from experiments and from thermodynamic modelling (White *et al.*, 2011). However, the comparison between experiments and thermodynamic calculations performed on the same compositions showed some differences regarding primarily the melt composition (White *et al.*, 2011). In addition, these approaches calculate melt composition at equilibrium with the solid residual assemblage, but kinetics may play an important role during crustal anatexis (*e.g.*, Acosta-Vigil *et al.*, 2010). Hence, studies of crustal melting currently involve a major unknown: the composition and volatile contents of primary anatectic melts in nature at the onset of crustal anatexis.

Recently, it has been shown that peritectic minerals in migmatitic granulites can trap tiny droplets of anatectic melt that formed by incongruent melting reactions (Cesare *et al.*, 2009). However, the geochemical and petrological "message" enclosed in these minute strongboxes still remains poorly intelligible (Clemens, 2009), mainly owing to the analytical difficulty in retrieving the original composition of the trapped melt, and to the lack of an extensive database on the anatectic melt inclusions (MI) composition. The re-assessment of many anatectic terranes worldwide (see Cesare *et al.*, 2011; Ferrero *et al.*, 2012) proved that the presence of MI hosted in peritectic minerals is the rule rather than an exception, opening the possibility for routine studies on the characterization of anatectic melts from different geodynamic settings.

In this thesis, taking advantage of a new experimental approach developed during this work for re-melting crystallized MI, a combined study of classical petrology and MI in migmatites was performed to characterize in detail the composition and the physical properties of anatectic melts, the fluid regimes, and the melting mechanisms and conditions during the anatexis of the metasedimentary crust located below the Ronda peridotite (Betic Cordillera, South Spain). Here, the tectonic emplacement of mantle rocks within the continental crust produced high-temperature metamorphism and partial melting in the underlying metasedimentary rocks (Tubia *et al.*, 1997).

PETROLOGY OF THE QUARTZO-FELDSPATHIC MIGMATITES

The petrologic study was made by petrographic observations, compositional characterization of minerals and bulk rocks, conventional thermobarometry and pseudosection calculations. The investigated migmatites are quartzo-feldspathic metatexites (Fig. 1a) located towards the base of the crustal sequence and quartzo-feldspathic mylonitic migmatites (Fig. 1b) found close to the contact with the peridotite. These migmatites are mainly composed of quartz+plagioclase+K-feldspar+biotite+sillimanite+garnet and probably derived from a greywacke protolith. Muscovite, very rare in the metatexites, is absent in the mylonites; graphite is present in all migmatites;

garnet and biotite contents are inversely correlated, *i.e.*, mylonites are much richer in garnet and poorer in biotite than metatexites. The former presence of melt is recorded by MI in garnet and melt pseudomorphs at the microscale, and by peraluminous leucogranitic leucosomes at the mesoscale.

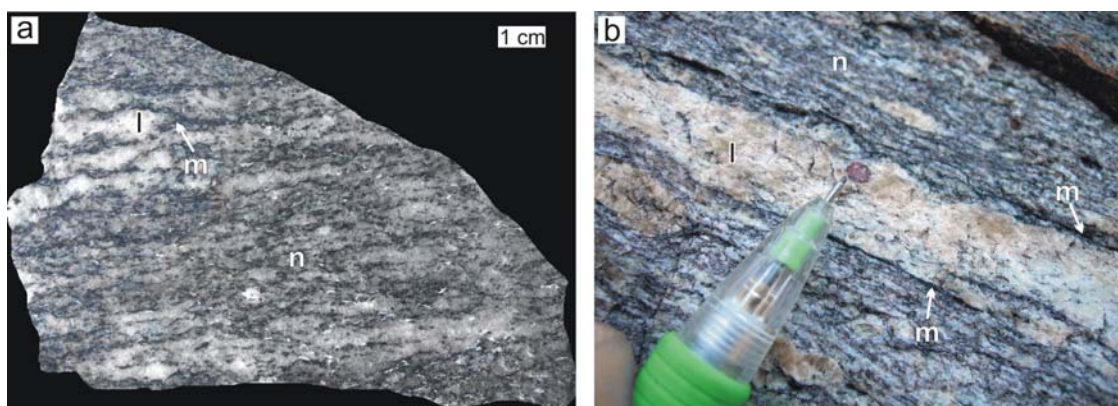


Fig. 1 - Investigated quartzo-feldspathic metatexites (a) and mylonitic migmatites (b) l: leucosome. n: neosome. m: melanosome.

The garnet-biotite geothermometry yields temperatures of 670-775 °C for metatexites and 660-970 °C for mylonites. The results for mylonites indicating $T \gg 900$ °C are clearly inconsistent with the phase assemblage. These scattered garnet-biotite temperatures likely indicate that garnet and biotite in the neosome of mylonites are not in equilibrium. Application of the Ti-in-biotite thermometer indicates temperature close to 700 °C for the prograde biotites in the metatexites, and temperatures in excess of 750 °C for most of the prograde biotites in mylonites. The GASP geobarometer yields pressures of 4.1-5.9 kbar for metatexites and 4.2-7.6 kbar for mylonites. Overall, the thermobarometric data indicate a decrease in temperature and pressure from the quartzo-feldspathic mylonites to the metatexites.

The phase equilibria in migmatites are sensitive to the bulk composition. Since the mineral phases in the metatexites are likely to constitute an equilibrium assemblage, a P-T pseudosection was constructed using the measured bulk composition of a metatexite (Fig. 2) to obtain a better understanding of the melting conditions and reactions.

Considering the assemblage stable during the anatexis of the rock (garnet + biotite + plagioclase + K-feldspar + sillimanite + quartz + melt) and the compositional isopleths of the MI-bearing garnet core and prograde biotite in the neosome, the pseudosection constrains the conditions of melting in the metatexites at $670 < T < 750$ °C and $3.5 < P < 5.5$ kbar.

These P-T estimates are consistent with the data obtained by thermobarometry. The petrographic features of the metatexites (*e.g.*, abundant biotite and fibrolite, the occurrence of very rare muscovite with resorbed shape and often armoured by K-feldspar, MI in peritectic garnet) along with the inferred melting conditions and the topology of the pseudosection (Fig. 2) indicate two feasible scenarios about melt-producing reactions in the metatexite: a) melting occurs first by the fluid-absent melting of muscovite closely followed by the continuous fluid-absent melting reaction of biotite or b) the first melting reaction encountered by the rock is the fluid-saturated solidus closely followed by the fluid-absent melting of biotite. The observed mineral assemblage in the mylonitic migmatites (*e.g.*, absence of muscovite, presence of Ti-rich prograde biotite, abundant sillimanite and MI in peritectic garnet) and the calculated melting temperature in excess of 750 °C, all indicate that the continuous biotite melting reaction was involved in the generation of melt in the mylonites.

The inferred melting reactions produced leucosomes with peraluminous leucogranitic compositions in both metatexites and mylonites. During cooling, H₂O in leucosome that exsolves from the crystallizing melts may diffuse into the residue (White & Powell, 2010) or be consumed by back reactions (Kriegsman, 2001), producing leucosomes with anhydrous or near-anhydrous chemical composition. Hence, leucosomes cannot

provide meaningful information about the fluid regime during the prograde melting. The detailed study of the MI in garnet will provide further clues on the nature of melting reactions and fluid regimes during the anatexis of these rocks.

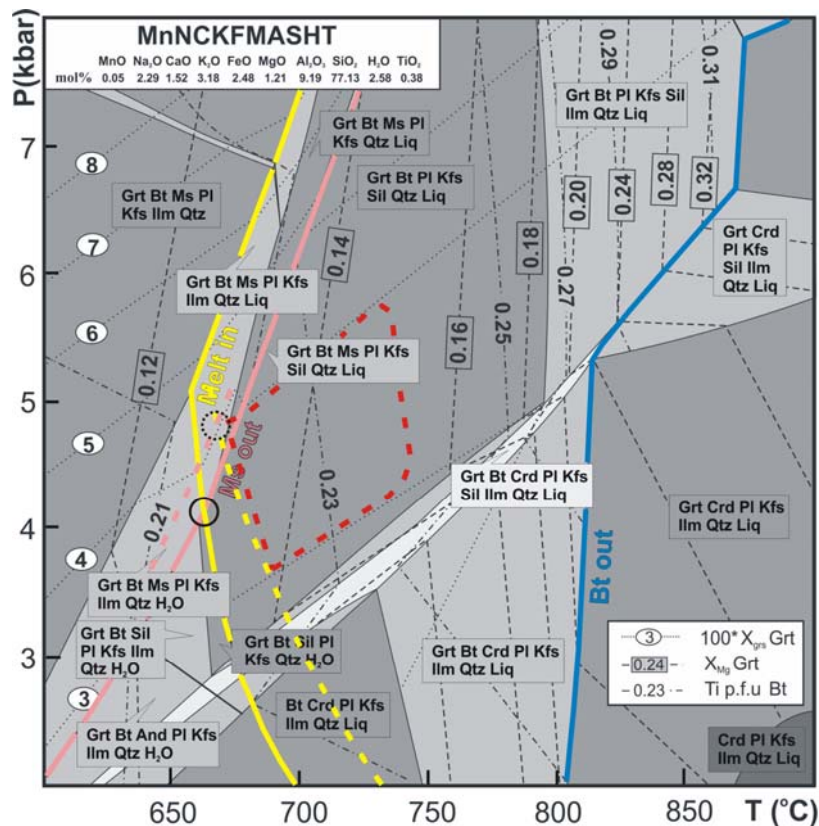


Fig. 2 - P-T pseudosection for the quartzo-feldspathic metatexites calculated in the MnNCKFMASHT system. Isopleths of garnet and biotite are reported. Yellow, pink and blue lines refer to the melt-in (*solidus*), muscovite-out and biotite-out curves, at $a_{H_2O} = 1$ (solid lines) and at $a_{H_2O} < 1$ (dashed lines). The red dashed area represents the P-T interval inferred for melting.

MELT INCLUSIONS IN THE QUARTZO-FELDSPATHIC MIGMATITES

Melt inclusions have been found in peritectic garnets of the investigated quartzo-feldspathic migmatites (Fig. 3).

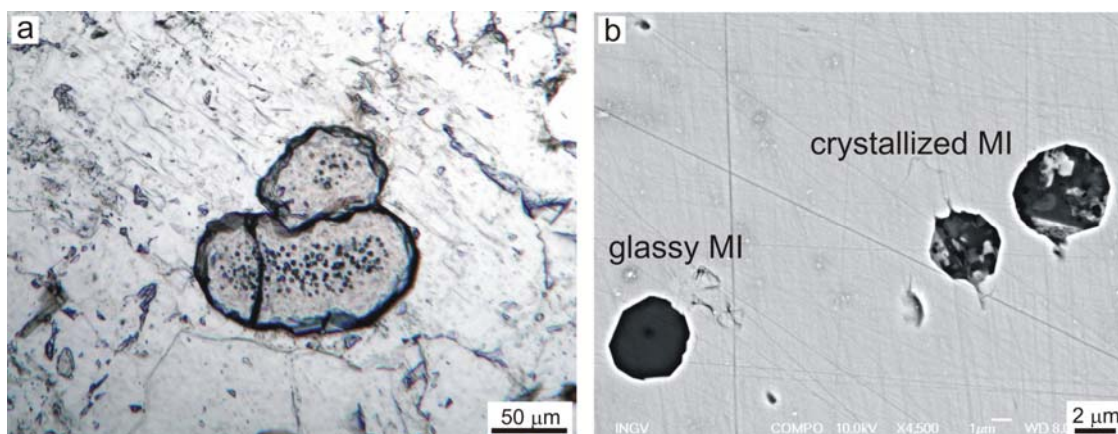


Fig. 3 - a) Small garnet crystals in metatexite with MI clusters at the core. b) FESEM BSE image of coexisting preserved glassy and crystal-bearing MI in mylonite.

A detailed study was carried out to characterize the microstructural features of melt inclusions and their chemical composition by microscope observation, FESEM imaging, ESEM X-ray elemental mapping, piston cylinder experimental remelting, Raman, and EMP analyses.

The inclusions are primary in origin and were trapped within peritectic garnet during crystal growth (Fig. 3a). They are very small in size, mostly $\leq 10 \mu\text{m}$, and typically show a well-developed negative crystal shape. Three types of inclusions were identified: totally crystallized (nanogranites), partially crystallized, and preserved glassy inclusions (Fig. 3b).

Crystallized melt inclusions contain a granitic phase assemblage with quartz, feldspars and micas (Fig. 4a and b). Some nanogranites display a variable micro- to nano-porosity that is greater in the samples from metatexites. Here, micro-Raman mapping of some crystallized MI located below the garnet surface documented the presence of micro- and nano-pores filled with liquid H_2O , suggesting H_2O exsolution during crystallization of hydrous melts to nanogranites. Some attempts to remelt crystallized MI with routine techniques, *i.e.*, the high-temperature microscope heating stage (Esposito *et al.*, 2012), produced extensive decrepitation and melt-host interaction, making samples unsuitable for a geochemical study (Cesare *et al.*, 2009).

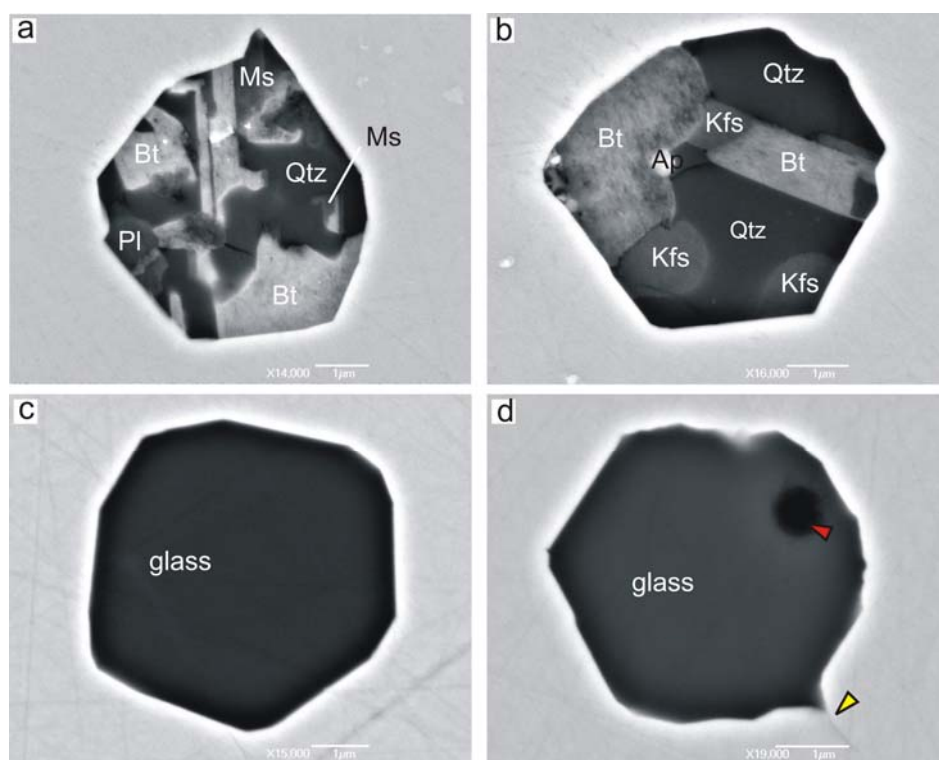


Fig. 4 – FESEM BSE images of nanogranites inclusions in metatexite (a) and mylonite (b) and of re-homogenized MI after piston cylinder experiments at 700 °C (c) and 800 °C (d). Red arrow: CO_2 bubble. Yellow arrow: decrepitation crack.

Hence, a new approach for the experimental re-homogenization of MI was developed, performing remelting experiments of MI from metatexites using a single-stage piston cylinder apparatus at 5 kbar and temperatures of 700, 750 and 800 °C for 24 h, both under dry and H_2O added conditions. At 700 °C, most MI are completely re-homogenized without dissolution of the host garnet (Fig. 4c).

Conversely, MI display decrepitation cracks and CO_2 bubbles when remelted at higher experimental temperatures (Fig. 4d). The absence of CO_2 bubbles in MI re-melted at 700 °C indicates that some CO_2 is dissolved into the melt of re-homogenized MI and that the new experimental approach is therefore crucial because it allows to maintain the primary high contents of fluid ($\text{H}_2\text{O}\pm\text{CO}_2$) in MI, that would otherwise be lost

during most of the homogenization experiments at ambient pressure (Bodnar & Student, 2006). The minimum re-homogenization temperature (700 °C) of nanogranites and partially crystallized MI from metatexites can be

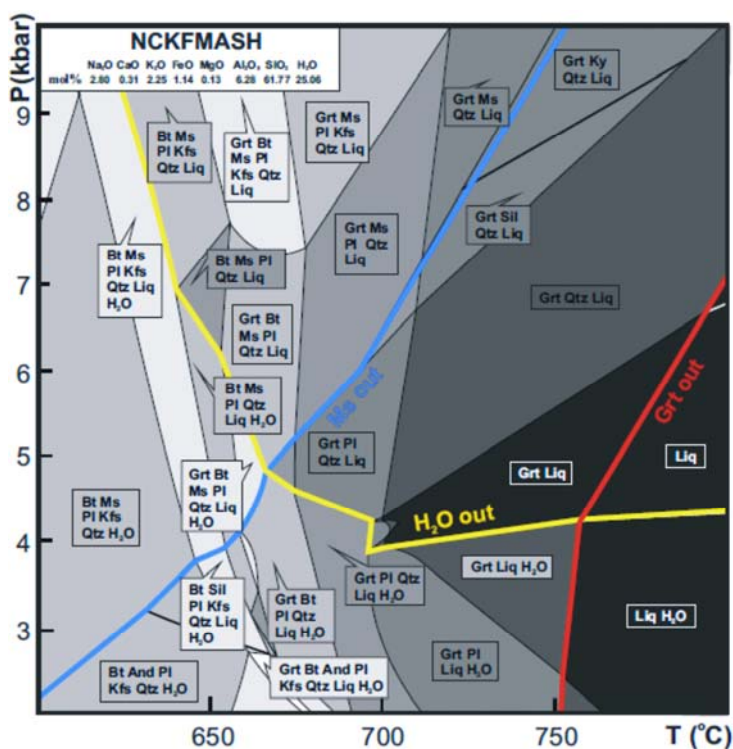


Fig. 5 - P-T pseudosection constructed using the composition of nanogranites in metatexite, remelted at 700 °C. Blue, yellow and red lines refer to the muscovite-, H₂O- and garnet-out curves, respectively.

assumed to be very close to the trapping temperature. The composition of MI re-homogenized at 700 °C is comparable to that of preserved glassy inclusions in the same rock. In general all the studied MI in the metatexites and mylonites have peraluminous leucogranitic compositions. However, inclusions in the mylonites (mostly glassy) display quite variable Na₂O/K₂O and have lower primary H₂O contents (1.0-2.6 wt.%) than MI in the metatexites (3.1-7.6 wt.%). For the first time, a pseudosection was constructed using the bulk composition of the fully re-homogenized MI from the metatexites (Fig. 5). The field for pure liquid starts at ~ 750 °C. However, this temperature is higher than the lowest temperature at which nanogranites have been experimentally remelted (700 °C). Instead, the temperature of 700 °C represents in the pseudosection the minimum temperature at which liquid coexists only with garnet (Fig. 5). Since the model for the melt phase used in these thermodynamic calculations was

made “to reflect more closely the total Fe + Mg and $X_{Fe} = Fe/(Fe + Mg)$ in experimental melts” as outlined by White *et al.* (2007), and given that experimental melts have lower FeO and MgO contents than the natural anatectic melts (*e.g.*, Lavaure & Sawyer, 2011), the field garnet+liquid in the pseudosection is likely a field in which only the liquid is stable until the minimum temperature of 700 °C (for a P ~ 4 kbar). The fully re-homogenization of nanogranites without garnet dissolution at 700 °C is a strong experimental evidence to this inference.

DISCUSSION

Combining information from the MI and from the classical petrology allowed a better understanding of the melting processes occurred in the crustal sequence below the Ronda peridotite. The data collected in this study suggest that the crustal melting at Ronda mainly occurred under H₂O-undersaturated conditions by the continuous biotite dehydration melting reaction and at temperatures that did not exceed ~ 800 °C. In the metatexites, towards the base of the crustal sequence, crustal anatexis likely started at the solidus (T ~ 700 °C) in presence of H₂O-rich intergranular fluids, considering (i) the occurrence of CO₂ in MI and graphite in the rock, (ii) that the devolatilization of hydrous phases produces graphite-saturated COH fluids characterized by maximum X_{H₂O} ~ 0.85 at ~ 5 kbar and ~ 700 °C and (iii) that the H₂O-saturation for granitic melts in equilibrium with COH fluids (with X_{H₂O} ~ 0.85) at 5 kbar is ~ 8 wt.%.

For the first time in the geologic literature, leucosomes and MI from the same migmatites have been analyzed and can be compared. On the Qtz-Ab-Or diagram (Fig. 6), normative compositions of the MI generally

plot close to the 5 kbar H₂O-undersaturated eutectic, whereas most of the leucosomes plot close to the Qtz-Or cotectic far away from the eutectic, suggesting that they may approach unmodified (*i.e.*, primary) anatectic melts that were produced at higher temperature conditions compared to the MI. Overall, MI record the evolution of melt composition during prograde anatexis, whereas leucosomes reflect the melt composition at, or closer to, the peak metamorphism conditions.

Using the major element compositions and H₂O contents as measured in re-homogenized MI, a melting temperature of 700 °C and the model proposed by Giordano *et al.* (2008), the viscosities of the anatectic melts produced at the onset of crustal anatexis in the metatexite are between 10^{4.8} and 10^{7.1} Pa s. These values are about two or three orders of magnitude greater than the viscosity considered for the low-T (< 750 °C) granitic melts in models on melt segregation and on deformation of the partially melted crust (10^{4.0} - 10^{4.9} Pa s; Scaillet *et al.*, 1996; Petford *et al.*, 2000), implying much greater rock strength and much longer timescales for melt extraction through the metasedimentary crust at Ronda.

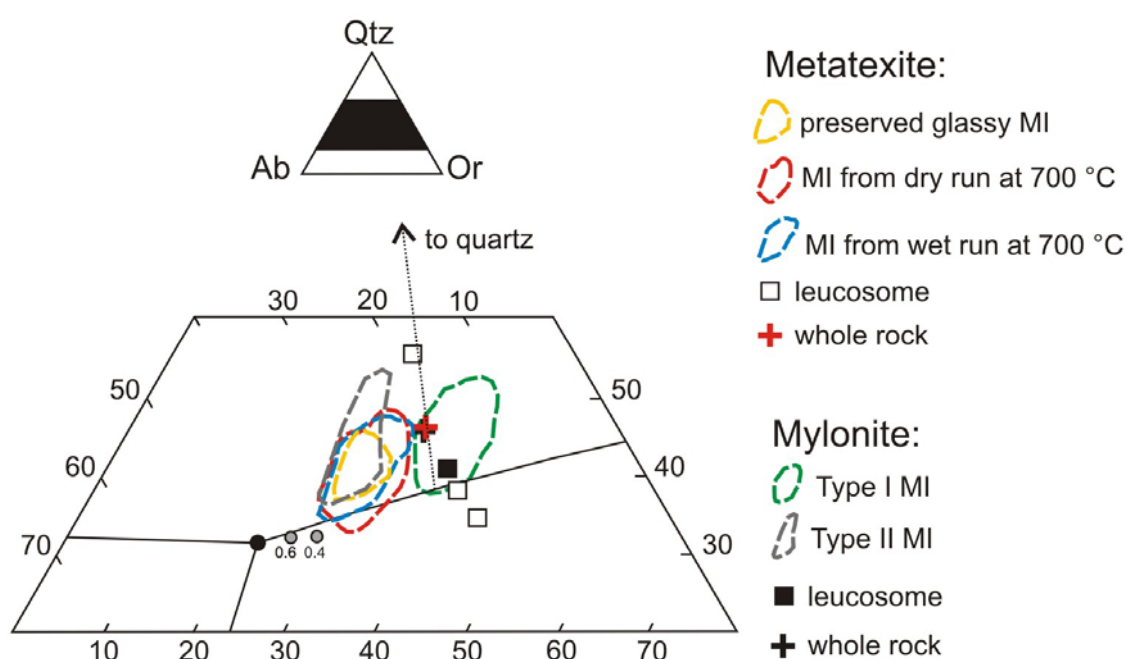


Fig. 6 - Normative compositions of the analyzed melts (MI and leucosomes) and whole migmatites, shown on the Qtz-Ab-Or diagram. Black arrow joins the whole rock compositions and the Qtz vertex. Black dot and lines refer to the eutectic point and cotectic lines for the subaluminous haplogranite system at 5 kbar and $a_{\text{H}_2\text{O}} = 1$; grey dots: eutectic points at $a_{\text{H}_2\text{O}} = 0.6$ and $a_{\text{H}_2\text{O}} = 0.4$ (Becker *et al.*, 1998).

CONCLUDING REMARKS

The present work, that represents the first combined study of MI and classical petrology on migmatites, shows that *in situ*, and otherwise impossible to retrieve, quantitative information on the earliest stages of crustal anatexis can be reliably gained from experimentally re-homogenized nanogranites and from preserved glassy MI in peritectic minerals from migmatites. Following the new experimental approach proposed in this study, the partially crystallized and nanogranite inclusions in peritectic garnets of migmatites from many orogenic belts worldwide can be successfully re-homogenized and then analyzed. Because the chemical variations in granitic rock suites are largely inherited from the source (Clemens & Stevens, 2012), the *in situ* characterization (*i.e.*, in the source region) of the first melt droplets produced at the onset of melting will be of paramount importance in

crustal petrology. Hereafter, it will be possible to determine the fluid regime during initial stages of S-type granite formation, rather than after the magma has separated from its source (see Clemens & Watkins, 2001), and the geochemical modelling on S-type granite magmatism and continental crust differentiation can now be constrained using directly measured natural primary melt compositions. The study of MI will also provide more realistic constraints to the strength of the partially melted crust and the timescales of melt extraction and ascent in anatectic terranes. Our data demonstrate that higher values for viscosity of low-T granitic melts should be considered in models on melt segregation, but also on deformation of the partially melted crust, because the first melt fractions (< 7%; Rosenberg & Handy, 2005) significantly affect the weakening of the continental crust.

REFERENCES

- Acosta-Vigil, A., Buick, I., Hermann, J., Cesare, B., Rubatto, D., London, D., Morgan, G.B. VI (2010): Mechanisms of crustal anatexis: a geochemical study of partially melted metapelitic enclaves and host dacite, SE Spain. *J. Petrol.*, **51**, 785-821.
- Becker, A., Holtz, F., Johannes, W. (1998): Liquidus temperatures and phase compositions in the system Qz-Ab-Or at 5 kbar and very low water activities. *Contrib. Mineral. Petrol.*, **130**, 213-224.
- Bodnar, R.J. & Student, J.J. (2006): Melt inclusions in plutonic rocks: petrography and microthermometry. In: "Melt inclusions in plutonic rocks", J.D. Webster, ed. *Mineral. Ass. Can., Short Course*, **36**, 1-26.
- Brown, M., Korhonen, F.J., Siddoway, C.S. (2011): Organizing melt flow through the crust. *Elements*, **7/4**, 261-266.
- Cesare, B., Ferrero, S., Salvioli-Mariani, E., Pedron, D., Cavallo, A. (2009): Nanogranite and glassy inclusions: the anatectic melt in migmatites and granulites. *Geology*, **37**, 627-630.
- Cesare, B., Acosta-Vigil, A., Ferrero, S., Bartoli, O. (2011): Melt inclusions in migmatites and granulites. In: "The Science of Microstructure - Part II", M.A. Forster & J.D. Fitz Gerald, eds. *J. Virt. Expl.*, **38**, paper 2, doi:10.3809/jvirtex.2011.00268.
- Clemens, J.D. (2003): S-type granitic magmas-petrogenetic issues, models and evidence. *Earth Sci. Rev.*, **61**, 1-18.
- Clemens, J.D. (2009): The message in the bottle: "Melt" inclusions in migmatitic garnets. *Geology*, **37**, 671-672.
- Clemens, J.D. & Stevens, G. (2012): What controls chemical variation in granitic magmas? *Lithos*, **134-135**, 317-329.
- Clemens, J.D. & Watkins, J.M. (2001): The fluid regime of high-temperature metamorphism during granitoid magma genesis. *Contrib. Mineral. Petrol.*, **140**, 600-606.
- Esposito, E., Klebesz, R., Bartoli, O., Klyukin, Y.I., Moncada, D., Doherty, A., Bodnar, R.J. (2012): Application of the Linkam TS1400XY heating stage to melt inclusion studies. *Centr. Eur. J. Geosc.*, doi: 10.2478/s13533-011-0054-y.
- Ferrero, S., Bartoli, O., Cesare, B., Salvioli-Mariani, E., Acosta-Vigil, A., Cavallo, A., Groppo, C., Battiston, S. (2012): Microstructures of melt inclusions in anatectic metasedimentary rocks. *J. Metam. Geol.*, **30**, 303-322.
- Giordano, D., Russell, J.K., Dingwell, D.B. (2008): Viscosity of magmatic liquids: a model. *Earth Planet. Sci. Lett.*, **271**, 123-134.
- Kriegsman, L.M. (2001): Partial melting, partial melt extraction and partial back reaction in anatectic migmatites. *Lithos*, **56**, 75-96.
- Lavaure, S. & Sawyer, E.W. (2011): Source of biotite in the Wuluma Pluton: replacement of ferromagnesian phases and disaggregation of enclaves and schlieren. *Lithos*, **125**, 757-780.
- Petford, N., Cruden, A.R., McCaffrey, K.J.W., Vigneresse, J.-L. (2000): Granite magma formation, transport and emplacement in the Earth's crust. *Nature*, **408**, 669-673.
- Rosenberg, C.L. & Handy, M.R. (2005): Experimental deformation of partially melted granite revisited: implications for the continental crust. *J. Metam. Geol.*, **23**, 19-28.
- Sawyer, E.W. (2008): Atlas of migmatites. *Can. Mineral., Spec. Publ.*, **9**, NRC Research Press, Ottawa, Canada. 371 p.
- Sawyer, E.W., Cesare, B., Brown, M. (2011): When the continental crust melts. *Elements*, **7/4**, 229-233.
- Scaillet, B., Holtz, F., Pichavant, M., Schmidt, M. (1996): Viscosity of Himalayan leucogranites: implications for mechanisms of granitic magma ascent. *J. Geophys. Res.*, **101/B12**, 27691-27699.
- Tubía, J.M., Cuevas, J., Ibarguchi, J.I.G. (1997): Sequential development of the metamorphic aureole beneath the Ronda peridotites and its bearing on the tectonic evolution of the Betic Cordillera. *Tectonophysics*, **279**, 227-252.
- White, R.W. & Powell, R. (2010): Retrograde melt-residue interaction and the formation of near-anhydrous leucosomes in migmatites. *J. Metam. Geol.*, **28**, 579-597.
- White, R.W., Powell, R., Holland, T.J.B. (2007): Progress relating to calculation of partial melting equilibria for metapelites. *J. Metam. Geol.*, **25**, 511-527.
- White, R.W., Stevens, G., Johnson, T.E. (2011): Is the crucible reproducible? Reconciling melting experiments with thermodynamic calculations. *Elements*, **7/4**, 241-246.